

# A short review on the synthesis, characterization, and application studies of poly(1-naphthylamine): a seldom explored polyaniline derivative

Sapana Jadoun<sup>1</sup> · Anurakshee Verma<sup>1</sup> · S. M. Ashraf<sup>1</sup> · Ufana Riaz<sup>1</sup>

Received: 7 March 2017 / Revised: 28 May 2017 / Accepted: 12 June 2017 / Published online: 4 July 2017  
© Springer-Verlag GmbH Germany 2017

**Abstract** Poly(1-naphthylamine) (PNA) has been one of the seldom explored polyaniline (PANI) derivatives in spite of its versatile electrochromic and optoelectronic properties. The present review summarizes, for the first time, synthesis, characterization, and application studies related to poly(1-naphthylamine) as well as its copolymers, blends, and nanocomposites that have been carried out during the past two decades. Details about the chemical as well as electrochemical techniques used for the synthesis of this polymer are provided along with various procedures adopted to improve its processibility via formulation of copolymers, blends, and nanocomposites. Recent studies dealing with the potential applications of this polymer in the field of catalysis and coatings are also evaluated.

**Keywords** Poly(1-naphthylamine) · Redox behavior · Nanocomposites · Copolymers · Photocatalysis

## Introduction

Polyaniline (PANI) has been one of the most extensively investigated conducting polymers because of its remarkable electrochromic behavior and diverse applications in the field of biosensors, coatings, electromagnetic shielding, etc. [1–6]. Although this polymer is thermally stable, it shows extremely poor solubility in common organic solvents [7–10]. The quest for development of soluble PANI derivatives has attracted the

attention of researchers towards polymerization of 1-naphthylamine (1-NPA) monomer which has fused benzene attached to aniline moiety (Fig. 1) [11–19].

In 1990, the possibility of polymerization of 1-NPA via electrochemical technique was first reported by Arévalo et al. [20]. In 1993, Moon et al. [21] first reported the chemical polymerization of 1-NPA using H<sub>2</sub>O<sub>2</sub> and Fe as catalysts. Since then, several investigations have been carried out pertaining to the synthesis and characterization of PNA and its copolymers as well as nanocomposites. Keeping in mind, the significance of this valuable PANI derivative and the fact that no review is available on PNA till date, the present article highlights the synthetic and application studies of PNA, that have been carried out for the past 20 years. The formulation of copolymers and nanocomposites of PNA has also been discussed along with their applications in field of sensors, photocatalysis, and corrosion protection.

## Chemical and electrochemical polymerization of micro poly(1-naphthylamine)

The electrocatalytic characteristics of PNA were reported in 1992 by Huang et al. [22]. They developed PNA films complexed with Ni(II) and Co(II) ions, but the formation of polymeric products was not confirmed. In 1995, Euler et al. [23] synthesized oligonaphthylamine films by electrochemical synthesis in aqueous medium containing potassium iodide. They obtained five different colored films showing variable redox behavior (Fig. 2). This was the first study that highlighted the redox properties of PNA. The as-synthesized green film revealed a peak at 850 nm along with a shoulder between 500 and 600 nm (Fig. 2).

A clear film was synthesized that exhibited no peak in the range of 400–1100 nm, while a blue film revealed a peak at 580 nm. Purple film of PNA showed a peak at 510 nm, while a pink film revealed maxima at 483 nm along with a tail moving

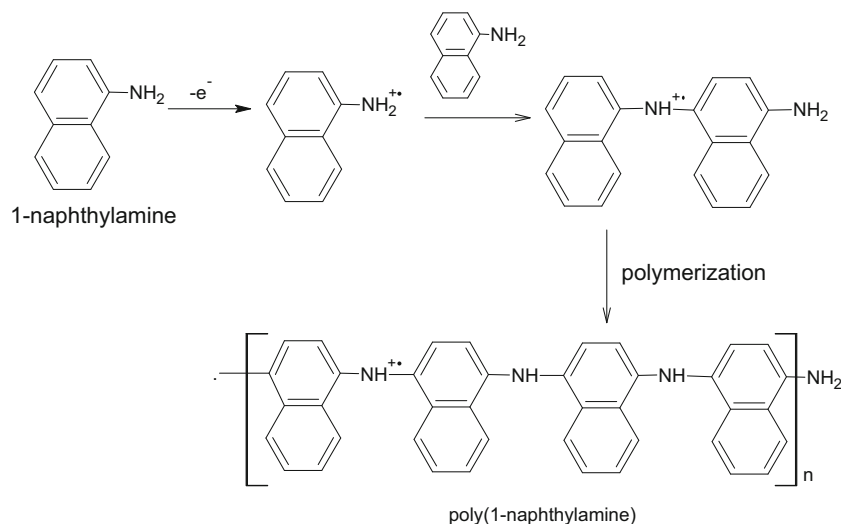
---

S.M. Ashraf is now retired

✉ Ufana Riaz  
ufana2002@yahoo.co.in

<sup>1</sup> Material Research Laboratory, Department of Chemistry, Jamia Millia Islamia, New Delhi 110025, India

**Fig. 1** Polymerization of 1-naphthylamine



towards the near-infrared (NIR) region. The chemical structures of the various redox states proposed by the authors are shown in Fig. 2. Shaffie [24] investigated a series of PNA films prepared in acetone/water mixture using different concentrations of

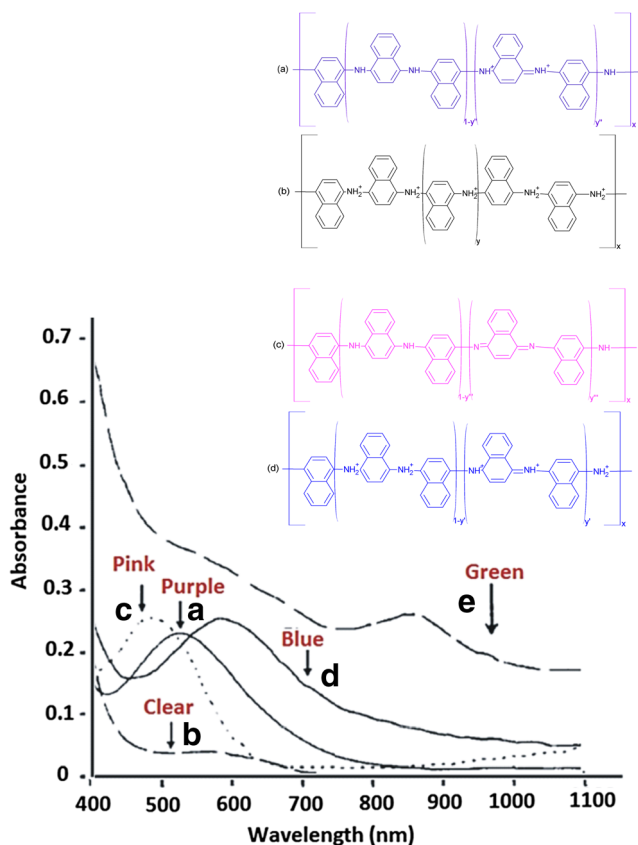


**Fig. 2** Visible spectra of the oligonaphthylamine films purple film ( $\lambda_{\max} = 510$  nm) (a), clear film ( $\lambda_{\max} = 580$  nm) (b), pink film ( $\lambda_{\max} = 483$  nm) (c), blue film ( $\lambda_{\max} = 580$  nm) (d), green film ( $\lambda_{\max} = 850$  nm) (e). Reprinted with permission from Elsevier Brian K. Schmitz, William B. Euler. Synthesis and characterization of oligonaphthylamines, *Journal of Electroanalytical Chemistry*, 399 (1995) 47–52

potassium persulfate as initiator. Although the polymerization mechanism was reported to be similar to that of PANI, the solubility of PNA was found to be superior to that of PANI. The specific conductance of the prepared polymers was found to be in the range of  $0.055\text{--}0.083 \Omega^{-1} \text{cm}^{-1}$ . The chemical structure of PNA was proposed to be planar as in the case of PANI.

Significant details about the regiochemistry of PNA were shown by Marjanovic et al. [25]. His group carried out the electrochemical polymerization of 1-NPA in the presence of acetonitrile/ $\text{LiClO}_4$  solution and compared the IR data with

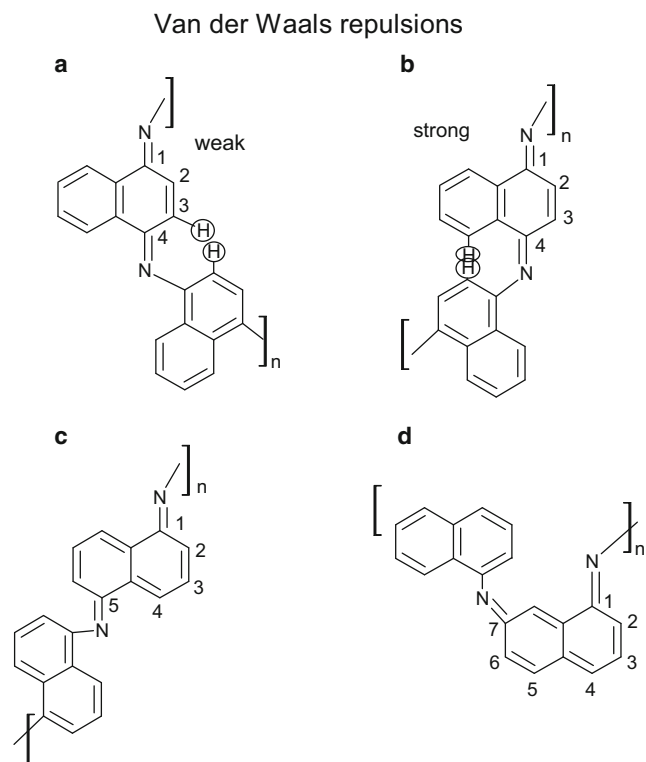
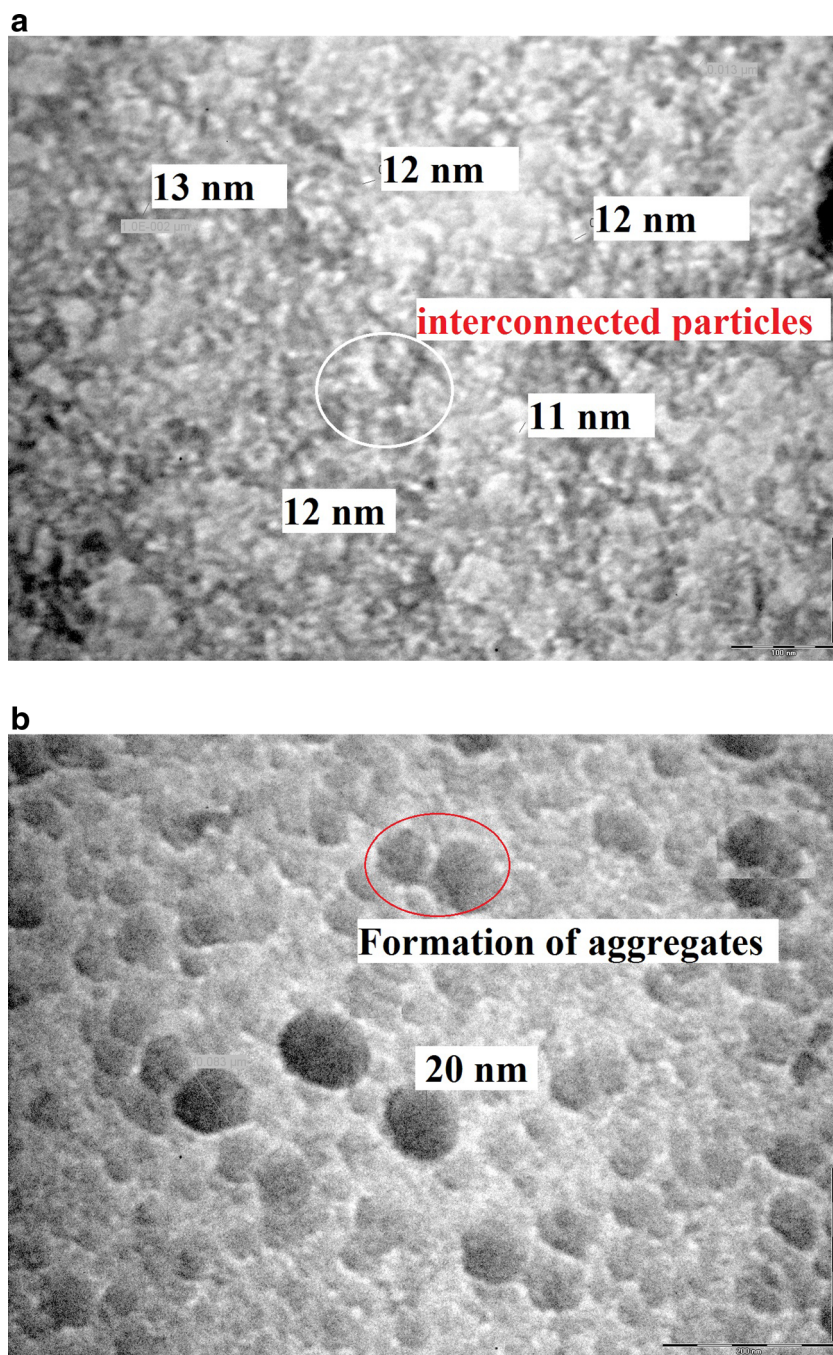


**Fig. 3** van der Waals repulsion caused by coupling of 1-naphthylamine dimer units through (a) N-C(4) linkage, (b) N-C(4) linkage, (c) N-C(5) linkage, and (d) N-C(7) linkage

**Fig. 4** TEM of chemically synthesized PNA **a** in the absence of HCl medium and **b** in the presence HCl medium. Reprinted with permission from Springer, Riaz, U.; Ahmad, S.; Ashraf, S.M. Effect of dopant on the nanostructured morphology of poly(1-naphthylamine) synthesized by template free method, *Nanoscale Res. Lett.* 2008, 3, 45



semiempirical quantum chemical calculations to determine the regiochemistry of PNA. The polymer products obtained were observed to be a mixture of N–C(4), N–C(5), and N–C(7) coupled units. The regioisomer of PNA shown in Fig. 3a was found to be a predominant product as weak van der Waals repulsions are created in this isomer which can be closely related to the regiochemistry of PANI. It was also proposed that the planarity of the oligomeric and polymeric oxidized forms of 1-NPA, coupled by the N–C(4) linkages, was hindered by strong steric repulsions as shown in Fig. 3b. It was also confirmed that when the dimer units exceed three units

(hexamer), stable planar structure was disrupted. Hence, the planar geometry was obtained only for structures coupled via N–C(5) linkages (Fig. 3c) and via N–C(7) linkages (Fig. 3d).

Various studies have been devoted towards designing PNA-modified glassy carbon electrodes (GCEs) for the detection of analytes which involve in situ electrochemical polymerization of NPA. A renewable and reproducible 1-NPA-modified carbon paste electrode was developed by Ojani et al. [26]. He incorporated  $\text{Ni}^{2+}$  ions into the PNA matrix using nickel chloride solution and used the system for electrocatalytic oxidation of various carbohydrates. The chronoamperometric results

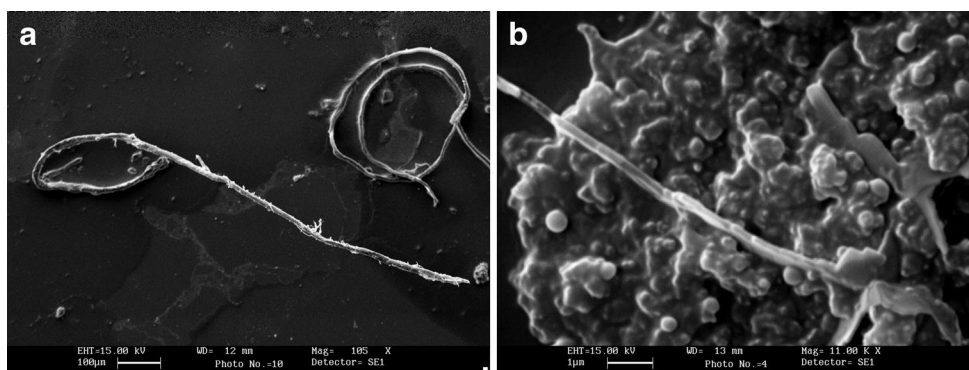


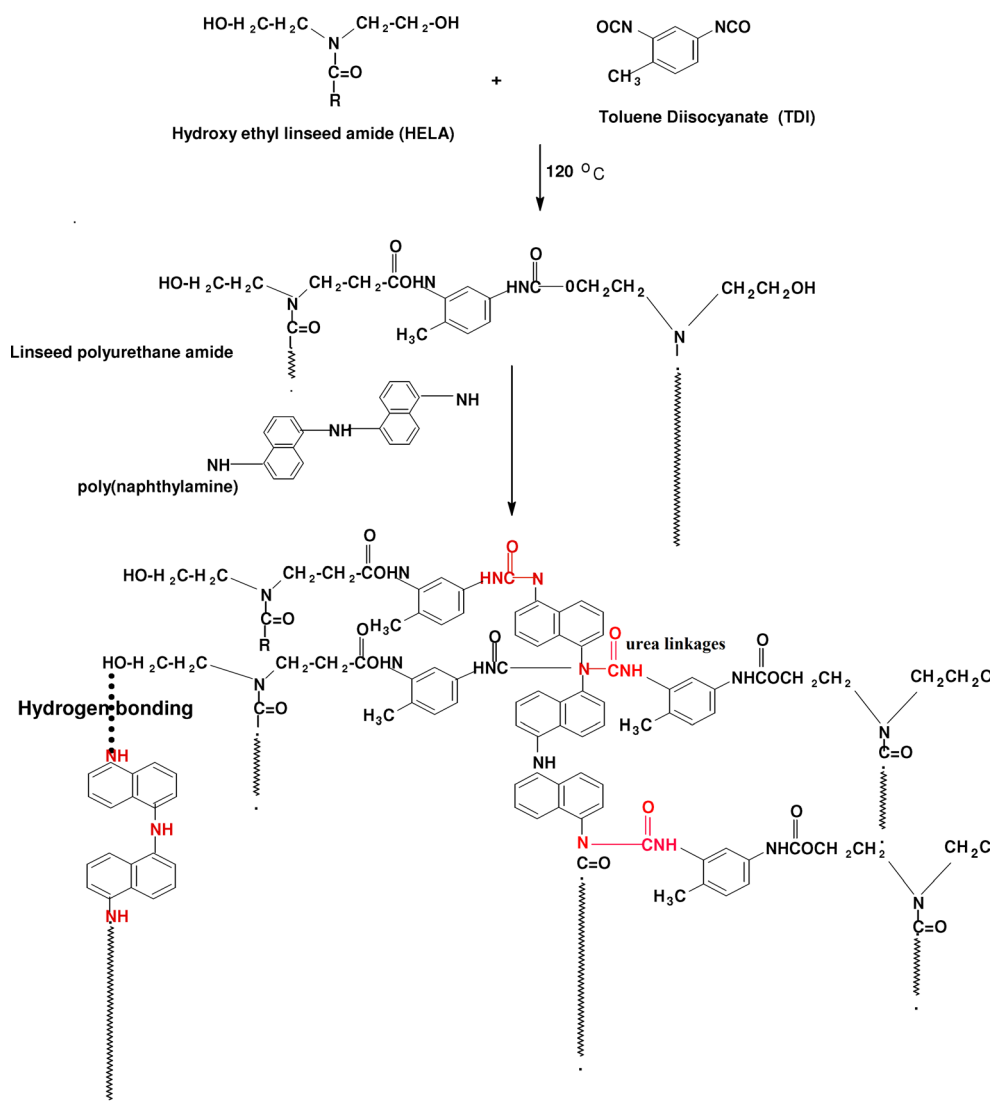
**Fig. 5** SEM of chemically synthesized PNA in methyl alcohol medium at subzero temperatures in the presence of **a** nitrogen environment and **b** oxygen environment. Reprinted with permission from Springer, Riaz, U.;

Ahmad, S.; Ashraf, S.M. Pseudo template synthesis of poly (1-naphthylamine): effect of environment on nanostructured morphology, *J.Nanopart. Res.* 2008, 10, 1209

showed that the *rate constant* values could overcome the kinetic limitations for carbohydrate oxidation by a catalytic process and therefore could largely reduce the overpotential for the oxidation reaction of carbohydrates.

Liu [27] also developed PNA-nickel (Ni(II)) modified GCE known as (PNA)-Ni/(GCE) via in situ electropolymerization of 1-naphthylamine at GCE, followed by incorporation of Ni(II) to polymeric layer by dipping the modified electrode in 1.0 M

**Fig. 6** Chemical structure of PNA/linseed oil-based polyurethane (LPUA) nanocomposite showing hydrogen bonding between NH group of PNA with urethane of LPUA and formation of urea linkages between urethane of LPUA with nitrogen of PNA. Reprinted with permission from Wiley, Ashraf, S.M.; S. Ahmad, Riaz, U. Development of novel conducting composites of linseed oil-based poly(urethane amide) with nanostructured poly(1-naphthylamine), *Polym. Int.* 2007, 56, 1173



nickel sulfate solution. The electrochromic characteristics were studied by cyclic voltammetry and chronoamperometry in alkaline media. Results revealed that the modified electrode showed electrocatalytic activity towards oxidation of formaldehyde. Arevalo et al. [28] designed PNA-copper-modified glassy carbon electrode which was amperometrically used for the detection of various carbohydrates. The results obtained were compared with Cu ion-modified electrode incorporated at open circuit. Results showed that the nucleation rate was limited by heterogeneous electron transfer process.

Lately, electrochemical determination of 2-(2-nitrophenyl)-1H-benzimidazole (NB) was carried out by Eramo et al. [29] using a PNA-modified glassy carbon electrode followed by an overoxidation treatment in 0.2 M sodium hydroxide solution. The electrochemical behavior of NB at the oxidized PNA electrode was investigated by cyclic voltammetry (CV) and square-wave voltammetry (SWV), and results showed that this electrode had a good response towards NB.

### Chemical synthesis of nanostructured poly(1-naphthylamine)

Nanostructures of conducting polymers such as nanorods, nanowires, nanofibers, and nanotubes combine the advantages of organic conductors with low-dimensional systems which can remarkably improve the physicochemical properties. Nanostructured PNA was first reported by Ashraf and coworkers [30] via template-free polymerization technique in alcoholic medium. The polymerization was confirmed by FTIR as well as UV-visible studies. Transmission electron microscopy (TEM) studies revealed that particle size was found to be in the range of 6–10 nm, while in presence of hydrochloric acid, PNA showed the tendency to undergo agglomeration and the particle size was increased up to 20–30 nm. It was argued that ethanol medium acted like a “pseudo template” and was responsible for obtaining a self-assembled morphology (Fig. 4). In another work, the same authors reported a “pseudo template approach” adopted for the synthesis of nanostructured PNA using cupric chloride as initiator in alcoholic medium [31]. In this case, the effect of atmospheric conditions was explored, and polymerization was carried out in the presence of N<sub>2</sub> and O<sub>2</sub>. It was reported that methanol acted as a pseudo template which facilitated the growth of self-assembled PNA nanoparticles in the presence of O<sub>2</sub> where granular agglomerates were formed (Fig. 5a), while nanofibers were obtained when polymerization occurred in N<sub>2</sub> environment (Fig. 5b). The results provided valuable information about controlling the morphology of nanostructured PNA.

Riaz et al. [32] also investigated template synthesis of nano-PNA using camphor sulfonic acid (CSA) in the presence

of three different initiators—benzoyl peroxide, ammonium persulfate, and potassium dichromate. FTIR confirmed the polymerization of 1-NPA through N–C(5) linkages, while dynamic light scattering data confirmed that the particle size of PNA varied between 115 and 117 nm. Conductivity was reported to be in the range of 10<sup>-3</sup> to 10<sup>-2</sup> S/cm.

### Studies on copolymerization of poly(1-naphthylamine)

Copolymerization is one of the most successful approaches to tailor the properties of polymers using various kinds of monomers having similar reactivity ratios. Electrochemical copolymerization has been widely adopted to synthesize several new conducting polymers showing remarkable enhancement in

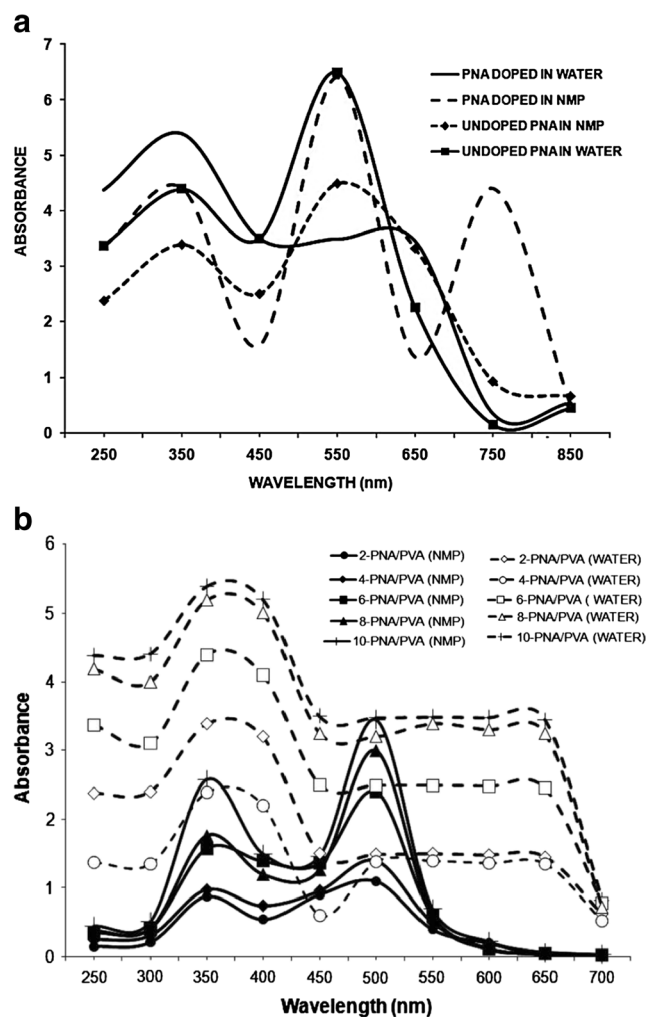


**Fig. 7** UV-visible spectra of **a** pure PNA (taken in NMP and water) and **b** PNA blends with poly(vinyl alcohol) (PVA) (taken in NMP and water). Reprinted with permission from Elsevier, Riaz, U.; Ahmad, S.; Ashraf, S.M. Effect of solvent on the characteristics of nanostructured composites of poly (1-naphthylamine) with poly (vinyl alcohol), *Curr.Appl.Phys.* 2009, 9, 581

conductivity, electrochemical activity, and thermal stability. Ashraf et al. [33] reported that the chemical copolymerization of 1-NPA with aniline (ANI) and *o*-toluidine (OTD) *co*-monomers and the effect of copolymerization were investigated using FTIR, UV-visible, X-ray diffraction (XRD), and TEM studies. The particle size of PNA was reported to be lower than the copolymers of PANI and poly(*o*-toluidine) (POT), being 50, 150, and 130 nm, respectively. XRD confirmed the semicrystalline nature of PNA, while the copolymers were reported to be amorphous. Massoumi et al. [34] also copolymerized 1-NPA and ANI, using ammonium persulfate as initiator in the presence of methane sulfonic acid (MSA). Variation in the morphologies of homopolymers and copolymers was confirmed by scanning electron microscopy (SEM) and was reported to occur due to the differences between the relative rates of interfacial nucleation and aqueous nucleation methods. The conductivity and solubility of copolymers were noticed to be 10–15 times higher than the copolymers prepared by conventional methods.

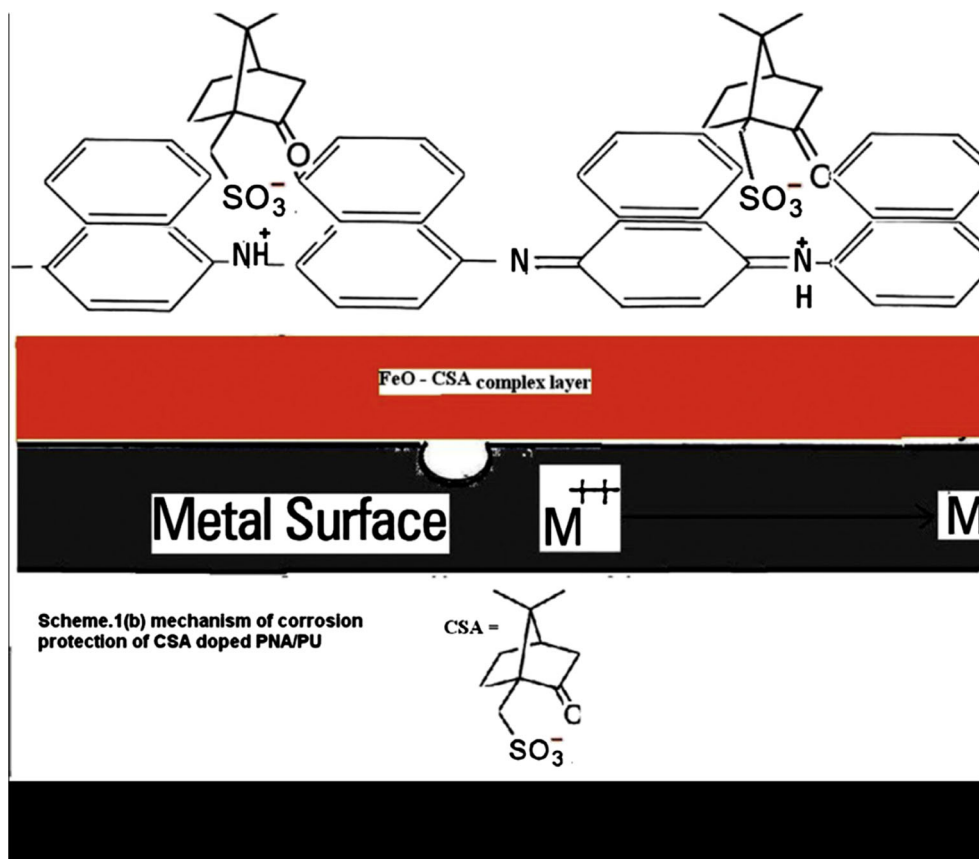
### Nanocomposites of poly(1-naphthylamine)

The design of blends and conducting nanocomposites offers a possibility of improving not only the processibility but also the pattern of distribution as well as control over the

dispersion of conducting polymer nanoparticles. Ashraf et al. [35] designed nanocomposites of PNA using different weight percent loadings varying between 0.5 and 2.5 wt% in linseed oil-based poly(urethane amide) (LPUA) matrix. Intense hydrogen bonding and the formation of urea-type linkages were confirmed by  $^1\text{H-NMR}$  results (Fig. 6). UV-visible studies revealed that even a small amount of PNA (as low as 0.5 wt%) in the composite showed polaronic bands. The interaction of PNA with LPUA molecules produced a slight blue shift in the spectra of the nanocomposite as compared to pure PNA. TEM of the nanocomposite revealed a homogeneous microstructure with particle size ranging from 17 to 27 nm. The same group synthesized nanocomposites of PNA with montmorillonite (MMT) by emulsion polymerization using three different oxidants [36]. The nanocomposite exhibited solubility in most of the organic solvents which was reported to be far superior in spite of lower loading of PNA in MMT (25 wt%). XRD revealed small expansion in the interlayer space of MMT due to longitudinal confinement of PNA chains. Conductivity values of PNA/MMT nanocomposites were found to be much higher than PANI-MMT nanocomposite due to ordered chain conformation of PNA that facilitated charge transfer.

Ashraf et al. [37] also synthesized nanocomposites prepared by loading of PNA (2–10 wt%) in poly(vinyl chloride) (PVC). The particle size of PNA/PVC composites was found

**Fig. 8** Mechanism of corrosion protection by camphor sulfonic acid (CSA) doped PNA/linseed oil polyurethane amide (LOPU) composite coatings through the formation of FeO-CSA complex layer that provides corrosion protection to the metal surface. Reprinted with permission from Elsevier, Riaz, U.; Ahmad, S.A.; Ashraf, S.M.; Ahmad, S. Effect of dopant on the corrosion protective performance of environmentally benign nanostructured conducting composite coatings, *Prog.Org.Coat.* 2009, 65, 405



to be in the range of 5–20 nm. At around 4 wt% loading of PNA in PVC, the conductivity value was found to be  $2.5 \times 10^{-2}$  S/cm due to the formation of self-assembled network of PNA nanoparticles in PVC matrix. The mechanical properties of nanocomposites having 8 and 10 wt% PNA, respectively, were found to be similar to that of low-density polyethylene (LDPE). Similarly, the authors synthesized PNA-dispersed polyvinyl alcohol (PVA) composites by loading 2–10 wt% PNA in aqueous as well as non-aqueous PVA media [38]. Uniform distribution of nanoparticles was reported for nanocomposites dissolved in water medium having particle size ranging between 5 and 30 nm, whereas a self-assembled network was attained in the case of nanocomposites synthesized in non-aqueous medium. The particle size was reported to be in the range of 10–65 nm. The variation in the properties of the nanocomposites in the two cases was due to solvent effect which caused intense hydrogen bonding (Fig. 7). It was corroborated that PVA accelerated dedoping of PNA in non-aqueous medium, while the nanocomposites synthesized in water exhibited good mechanical properties and electrical conductivity. Anbarasan et al. [39] chemically polymerized 1-NPA and loaded different nanosized metal oxides  $\text{Sb}_2\text{O}_3$ ,  $\text{CrO}_3$ ,  $\text{V}_2\text{O}_5$ ,  $\text{Al}_2\text{O}_3$ ,  $\text{As}_2\text{O}_3$ , and ammonium heptamolybdate (AHM). The presence of benzenoid and quinonoid rings in PNA was confirmed by the FTIR

spectroscopy, while TEM showed the presence of 25–40 nm metal oxide particles in the PNA matrix.

## Application studies of PNA

Although remarkable optoelectronic characteristics and superior processibility have been reported for PNA and its nanocomposites, there are only few studies available in literature dealing with the application studies of this remarkable PANI derivative. Initially, few investigations were reported dealing with the sensing capability of this polymer which has been discussed in the synthesis part. The proceeding section will cover the studies that have been reported by some authors in the field of corrosion-resistant coatings and water remediation using PNA.

## Corrosion-resistant coatings of poly(1-naphthylamine) and its antibacterial studies

A number of studies were reported in the mid-1990s pertaining to the potential application of conducting polymers as corrosion inhibitors. In 2007, Ahmad et al. [40] developed PNA-based waterborne protective using resorcinol formaldehyde (RF) and PVA. The corrosion protective performance

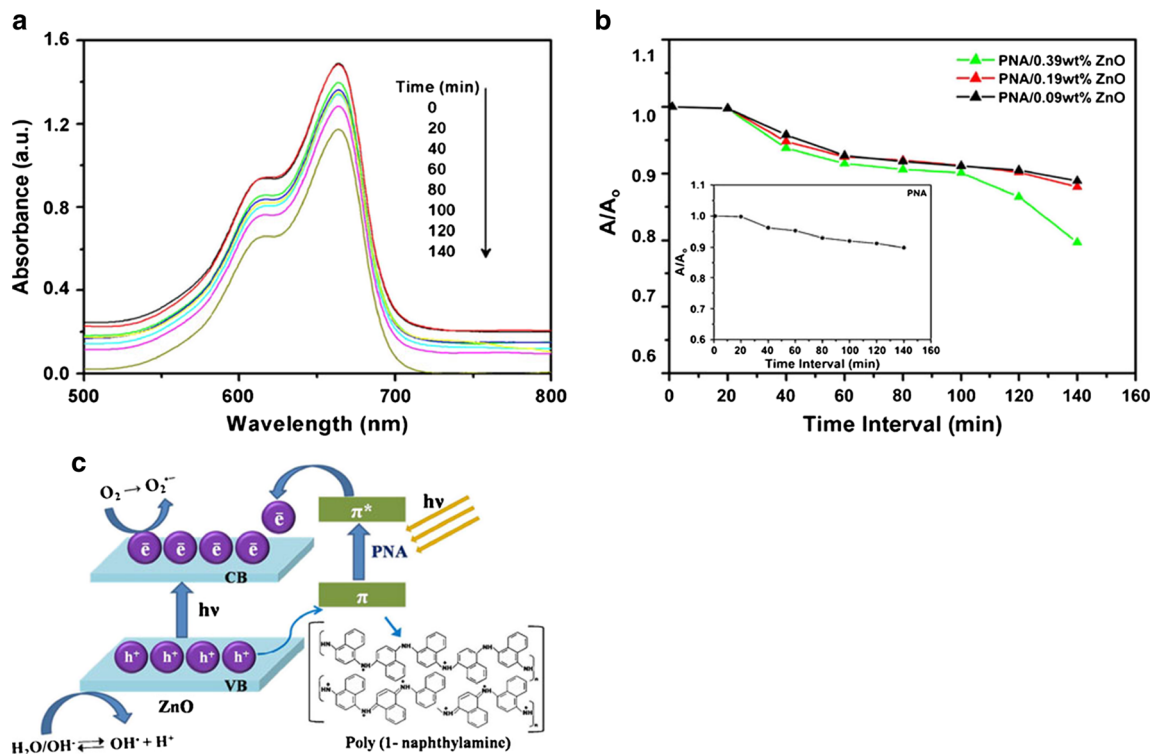


**Fig. 9** **a** UV-Vis absorbance spectra of decomposed MB dye solution by visible light over PNA/0.39 wt% ZnO nanocomposite. **b** Extent of decomposition of MB dye with respect to time intervals over pristine PNA and PNA/ZnO nanocomposites. **c** A schematic illustration of photocatalytic activity of PNA/ZnO nanocomposite. *Inset of b* shows

the degradation rate of MB dye over pristine PNA Reprinted with permission from Springer, Ameen, S.; Akhtar, S.; Kim, Y.S. Synthesis and characterization of novel poly(1-naphthylamine)/zinc oxide nanocomposites: application in catalytic degradation of methylene blue dye, *Coll.Polym.Sci.*2010, 288, 1633

was investigated on mild steel (MS) by determining the corrosion protective efficiency and corrosion resistance in acid, alkaline, and saline media via open circuit potential (OCP) measurements. The morphologies of coated, uncoated, as well as corroded samples were analyzed by SEM. Superior corrosion protective performance was observed which was compared to the reported solvent-based conductive polymer coatings in different corrosive media. It was shown that PNA/PVA/RF acted as “barrier composite coatings” and prevented the permeation of corrosive ions due to the presence of a compact morphology. It was also shown that in the presence of corrosive medium, PNA exhibited oxidized state, which was able to passivate MS for several days. The same authors [41] also developed nanocomposite coatings of CSA-doped PNA with linseed oil polyurethane (LOPU), and the corrosion resistance performance was compared with PANI-based polyurethane coatings. The composite coatings of CSA-doped PNA dispersed in LOPU matrix (CSA-PNA/LOPU) were found to exhibit promising corrosion resistance performance. The dispersion of CSA-PNA in LPOU was noticed to be more homogeneous, which facilitated the formation of well adherent, uniform, dense, and continuous passive film that prevented the attack of the corrosive species on mild steel (Fig. 8).

Riaz et al. [42] also reported the antibacterial activity of PNA and its copolymers, with aniline and *o*-toluidine in *N*-methyl pyrrolidone (NMP) solvent against *Escherichia coli* and *Staphylococcus aureus* using ampicillin as the control drug. The activity of PNA was found to be superior to that of the control drug against *E. coli*, while for *S. aureus*, it was comparable to that of the control drug. The antimicrobial activity of the copolymer of PNA with PANI showed higher activity than both PNA and the control drug, whereas the copolymer of PNA with POT revealed the highest antimicrobial activity against both bacterial stains. The chemical nature and nanostructure of PNA copolymers were found to significantly influence the antibacterial activity.

### Catalytic activity of poly(1-naphthylamine) and its nanocomposites

Photocatalytic degradation has been widely reported as a facile technique to decompose organic pollutants into non-toxic fragments. The combination of inorganic semiconductors such as ZnO and TiO<sub>2</sub> with conducting polymers has been reported to remarkably enhance the photocatalytic activity due to slow recombination rate of charges during electron transfer processes and good thermal stability. In this regard, Shin et al. [43] investigated the photocatalytic activity of PNA/ZnO nanocomposites using methylene blue (MB) as a model dye. It was reported that the surface properties of PNA molecules were altered by adding ZnO particles and a prominent red shift in the UV-Vis absorption spectra of the

nanocomposites was noticed which showed that they exhibited photocatalytic properties by absorbing photons under visible light irradiation. MB dye was degraded by 22 wt% over the surface of these nanocomposites due to high charge separation of electron (e<sup>-</sup>) and hole (h<sup>+</sup>) pairs in the excited states of coupled PNA and ZnO particles (Fig. 9).

The mechanism of photocatalytic activity in PNA/ZnO nanocomposites was explained on the basis of creation of photoexcited electrons (e<sup>-</sup>) through electron transfer into conduction band (CB) of ZnO from the π\* orbital of PNA molecules, while the formation of holes took place by transfer of electrons from valence band (VB) of ZnO to π orbital of PNA (Fig. 9). The holes (h<sup>+</sup>) generated in the VB of ZnO reacted

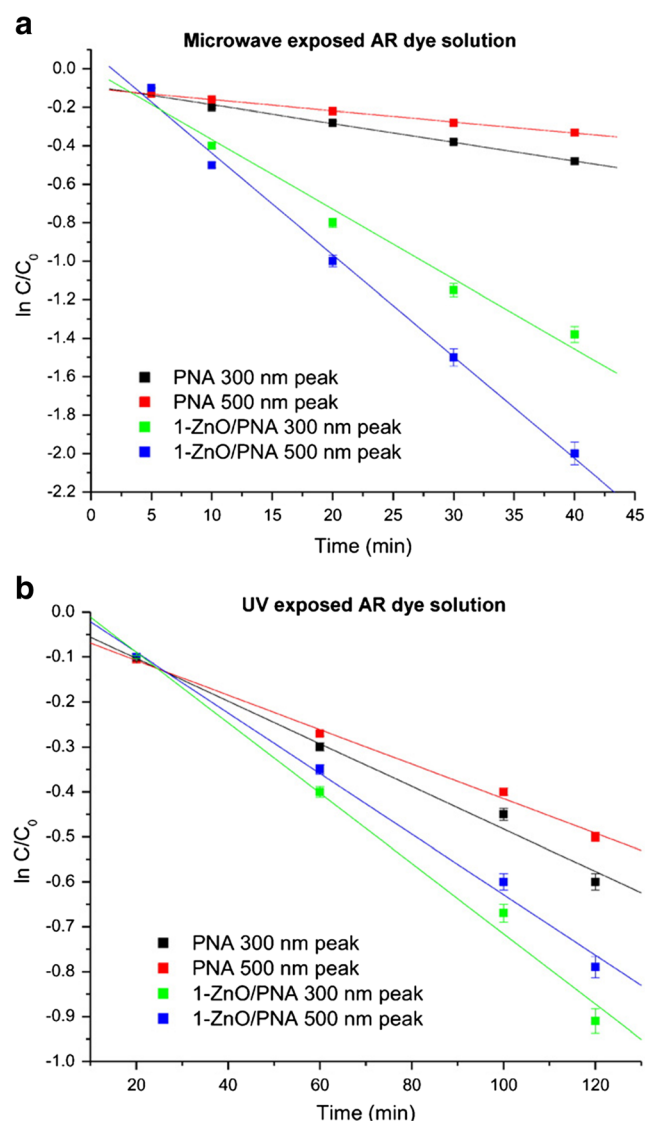


**Fig. 10**  $\ln C/C_0$  vs. time plot for degradation of alizarin red (AR) dye solution containing PNA and 1-ZnO/PNA as catalyst when exposed to **a** microwave irradiation and **b** UV irradiation. Reprinted with permission from Elsevier, Riaz, U.; Ashraf, S.M.; Budhiraja, V.; Aleem, S.; Kashyap, J. Comparative studies of the photocatalytic and microwave-assisted degradation of alizarin red using ZnO/poly(1-naphthylamine) nanohybrids, *J.Mol.Liq.* 2016, 216, 259



with hydroxyl radicals to generate  $\text{OH}^\bullet$  free radical. The charge separation of  $e^-$ - $h^+$  pairs facilitated the formation of oxy-radicals and hydroxyl radicals.

Riaz et al. [44] also investigated photocatalytic activity of ZnO/PNA nanocomposites against alizarin red (AR) dye and compared their results with the microwave-assisted catalytic activity of the same nanocomposite. The morphological investigation of the nanocomposites confirmed the formation of core shell morphology with particle size ranging between 20 and 45 nm. It was reported that as compared to UV irradiation, the rate of degradation was faster under microwave irradiation, and 90% degradation was achieved within 40 min. Although both techniques revealed kinetics of degradation, the *rate constant* ( $k$ ) values were noticed to be 0.052 and 0.036, respectively, for the 300 and 500-nm peaks of AR dye when degraded under microwave, while they were reported to be 0.009 and 0.007 under UV irradiation (Fig. 10). The  $\bullet\text{OH}$  radical generation was found to increase remarkably for dye solutions exposed to microwave irradiation.

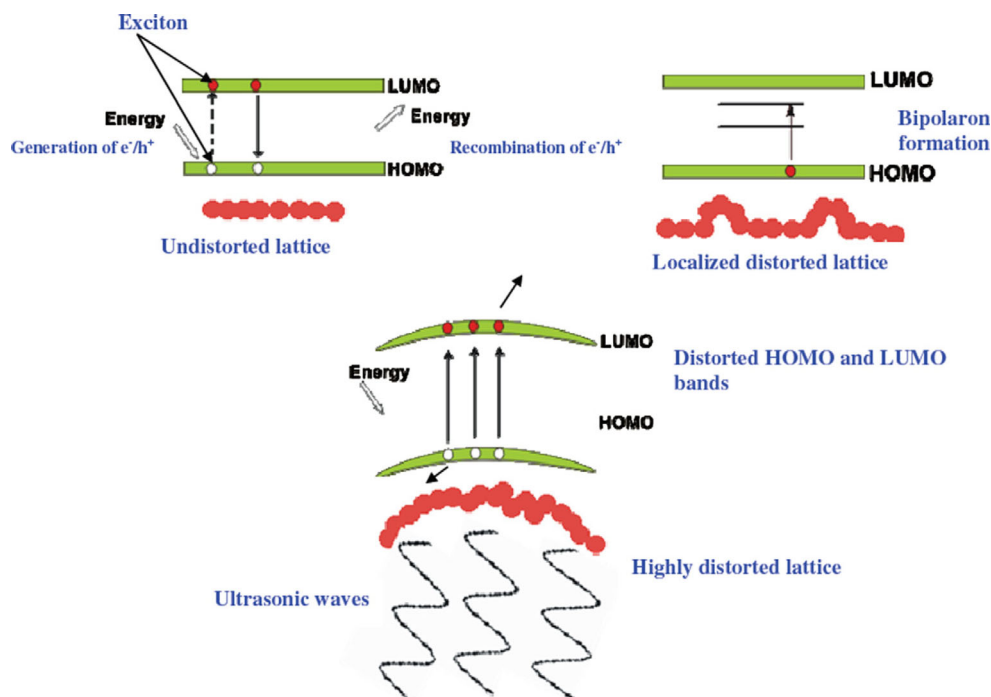
Riaz and Ashraf [45] also studied the photocatalytic behavior of pure PNA nanotubes under solar irradiation using Comassie blue (CB) dye. Ultrasonic irradiation was found to accelerate the photodegradation and mineralization of CB dye. Sonophotocatalysis exhibited pseudo-first-order rate kinetics.

It was explained that when PNA is excited by sufficient energy under visible light irradiation, electrons from valence band of PNA jump to the conduction band. The creation of holes in the valence band obviates  $e^-/h^+$  recombination (Fig. 11). Sonication was shown to cause fast mass transport that prevented  $e^-/h^+$  recombination, while  $e^-$  in the conduction band reacted with  $\text{O}_2$  as well as  $\text{H}_2\text{O}$  molecules sticking at the

surface of PNA particles and formed free radicals. The  $h^+$  oxidized water molecules to form  $\text{H}^+$  and  $\text{OH}^-$  free radicals and degraded the dye in solution.

Riaz and Ashraf [46] also studied the catalytic activity of PNA under microwave irradiation to degrade and mineralize Orange G (OG) dye. PNA as a microwave catalyst was found to enhance the dye degradation by almost two times, and OG dye solution was found to degrade up to 90 wt% in 20 min at  $30^\circ\text{C}$  in the presence of PNA. The same solution revealed mineralization up to 85% in 40 min as confirmed by the total organic content (TOC) analysis. The same authors also investigated the degradation of methyl orange (MeO) in neutral, acidic, and basic media under microwave irradiation using PNA nanotubes as catalyst in the absence of any light source [47, 48]. The degradation of the dye in the presence of PNA catalyst and in acidic, basic, and neutral media followed first-order rate kinetics. Rate constant,  $k$ , values were found to be slightly dependent on the pH of the dye solutions. Liquid chromatography-mass spectroscopy analysis confirmed that dye degraded into smaller fragments of low molar masses. Bagheri et al. [49] synthesized  $\text{Fe}_3\text{O}_4$  containing nanocomposites of PNA and PANI copolymers via chemical oxidative polymerization, and SEM revealed that the copolymer possessed a porous structure with diameter less than 50 nm. The nanocomposite was evaluated for its adsorption capacity against rhodamine B dye, and it was found that it showed a higher extraction efficiency due to porous morphology of the copolymer. Lately, Tran et al. [50] also studied the activity of PNA- $\text{Fe}_3\text{O}_4$  nanocomposites for As(III) wastewater remediation. The PNA/ $\text{Fe}_3\text{O}_4$  size varied from 25 to 30 nm measured by SEM, while room temperature vibrating sample

**Fig. 11** Behavior of PNA as a photocatalyst when exposed to ultrasonic irradiation showing lattice distortion and formation of bipolarons that prevent electron-hole recombination. Reprinted with permission from Elsevier, Riaz, U.; Ashraf, S.M. Latent photocatalytic behavior of semiconducting poly(1-naphthylamine) nanotubes in the degradation of Comassie Brilliant Blue RG-250, Sep.Purf.Technol. 2012, 95, 97



magnetometer (VSM) measurements revealed that the saturation magnetic moment of PNA/Fe<sub>3</sub>O<sub>4</sub> decreased as PNA concentration increased from 5 to 15 wt%. The arsenic adsorption capacity of the PNA/Fe<sub>3</sub>O<sub>4</sub> with 5 wt% PNA was reported to be better than that of Fe<sub>3</sub>O<sub>4</sub> in neutral media.

## Conclusion

Various polymerization strategies have been reported for the synthesis of microstructured and nanostructured PNA. The physical and chemical properties reported by different authors reveal that it is superior to PANI in terms of processibility and environmental stability. Although nanocomposites and copolymers of PNA have been widely reported, the application studies of this polymer as cited in the literature are mostly limited to its utilization as a photocatalyst and as filler in corrosion-resistant coatings. We believe that there is still a lot of scope in exploring the optoelectronic applications of this polymer for its application in organic light-emitting diodes (OLEDs). We hope that this review would help researchers working in this area to explore new avenues for this magnificent PANI derivative.

**Acknowledgements** The corresponding author Dr. Ufana Riaz wishes to acknowledge the DST-SERB for granting major research project vide sanction number SB/S1/PC-070/2013. One of the coauthor Mrs. Sapana Jadoun also wishes to acknowledge the DST-SERB for Senior Research Fellowship (SRF) under the same project.

## Compliance with ethical standards

**Conflict of interest** The authors declare they have no conflict of interest.

## References

- Xu D, Fan L, Gao L, Xiong Y, Wang Y, Ye Q, Yu A, Dai H, Yin Y, Cai J, Zhang L (2016) Micro-nanostructured polyaniline assembled in cellulose matrix via interfacial polymerization for applications in nerve regeneration *ACS Appl Mater Interf* 8(27):17090–17097
- Pramanik N, Dutta K, Basu RK, Kundu PP (2016) Aromatic  $\pi$ -conjugated Curcumin on surface modified polyaniline/polyhydroxyalkanoate based 3D porous scaffolds for tissue engineering applications *ACS Biomater Sci Engg* 2(12):2365–2377
- Kumari P, Khawas K, Nandy S, Kuila BK (2016) A supramolecular approach to polyaniline graphene nanohybrid with three dimensional pillar structures for high performing electrochemical supercapacitor applications *Electrochim Acta* 190(1):596–604
- Marmisollé WA, Azzaroni O (2016) Recent developments in the layer-by-layer assembly of polyaniline and carbon nanomaterials for energy storage and sensing applications. From synthetic aspects to structural and functional characterization *Nano* 8:9890–9918
- Khan A, Khan AAP, Rahman MM, Asiri AM (2016) High performance polyaniline/vanadyl phosphate (PANI-VOPO<sub>4</sub>) nano composite sheets prepared by exfoliation/intercalation method for sensing applications *Eur Polym J* 75:388–398
- Patel HA, Patel AL, Bedekar AV (2016) Polyaniline coated on celite, a heterogeneous support for palladium: applications in catalytic Suzuki and one-pot Suzuki–aldol reactions *New J Chem* 40:8935–8945
- Salavagione HJ (2016) Preparation and characterization of “clickable” polyaniline derivatives on graphene modified electrodes *J Electroanal Chem* 765(15):118–125
- Abidi M, Bernabeu SL, Huerta F, Montilla F, Hentati SB, Morallon E (2016) The chemical and electrochemical oxidative polymerization of 2-amino-4-tert-butylphenol *Electrochim Acta* 212:958–965
- Gazotti Jr WA, Faez R, De Paoli M-A (1999) Thermal and mechanical behaviour of a conductive elastomeric blend based on a soluble polyaniline derivative *Eur Polym J* 35(1):35–40
- Alva KS, Kumar J, Marx KA, Tripathy SK (1997) Enzymatic synthesis and characterization of a novel water-soluble polyaniline: poly (2,5-diaminobenzenesulfonate) *Macromolecules* 30(14):4024–4029
- Hu J, Shao D, Chen C, Sheng G, Ren X, Wang X (2011) Removal of 1-naphthylamine from aqueous solution by multiwall carbon nanotubes/iron oxides/cyclodextrin composite *J Hazard Mater* 185(1):463–471
- Ikeda M, Shimada K, Sakaguchi T (1983) High-performance liquid chromatographic determination of free fatty acids with 1-naphthylamine *J Chromatography B: Biomed Sci Appl* 272:251–259
- Li Z, Sun S, Qiao H, Yang F, Zhu Y, Kang J, Wu Y, Wu Y (2016) Palladium-catalyzed regioselective C8–H amination of 1-naphthylamine derivatives with aliphatic amines *Org Lett* 18(18):4594–4597
- Hou L, Zhu D, Wang X, Wang L, Zhang C, Chen W (2013) Adsorption of phenanthrene, 2-naphthol, and 1-naphthylamine to colloidal oxidized multiwalled carbon nanotubes: effects of humic acid and surfactant modification *Environ Toxicol Chem* 32(3):493–500
- Ghosh K, Rathi S, Kushwaha R (2013) Sensing of Fe(III) ion via turn-on fluorescence by fluorescence probes derived from 1-naphthylamine *Tetrahedron Lett* 54(48):6460–6463
- Vettorazzi N, Silber JJ, Sereno L (1981) Anodic oxidation of 1-naphthylamine in acetonitrile *J Electroanal Chem Interf Electrochem* 125(2):459–475
- Hassan SSM, Marzouk SAM, Sayour HEM (2003) Selective potentiometric determination of nitrite ion using a novel (4-sulphophenylazo)-1-naphthylamine membrane sensor *Talanta* 59(6):1237–1244
- Kirby AJ, Percy JM (1988) Synthesis of 8-substituted 1-naphthylamine derivatives. Exceptional reactivity of the substituents *Tetrahedron* 44(22):6903–6910
- Radomski JL, Deichmann WB, Altman NH, Radomski T (1980) Failure of pure 1-naphthylamine to induce bladder tumors in dogs *Cancer Res* 40:3537–3539
- Arévalo AH, Fernández H, Silber JJ, Sereno L (1990) Mechanism of electropolymerization of 1-naphthylamine in aqueous acid media *Electrochim Acta* 35(4):741–748
- Moon DK, Osakada K, Maruyama T, Kubota K, Yamamoto T (1993) Synthesis of poly (1-aminonaphthalene) and poly (1-aminoanthracene) by chemical oxidative polymerization and characterization of the polymers *Macromolecules* 26:6992–6997
- Huang S-S, Lin H-G, Yu R-Q (1992) Electrocatalysis of a chemically modified poly (1-naphthylamine) film electrode *Anal Chim Acta* 262(2):331–337
- Schmitz BK, Euler WB (1995) Synthesis and characterization of oligonaphthylamines *J Electroanal Chem* 399(1–2):47–52
- Shaffie KA (2000) Preparation and characterization of polynaphthyl amine (PNA) as a novel conducting polymer *J Appl Polym Sci* 77(5):988–992

25. Marjanovic GC, Marjanovic B, Stamenkovic V, Vitnik Z, Antic V, Juranic I (2002) Structure and stereochemistry of electrochemically synthesized poly-(1-naphthylamine) from neutral acetonitrile solution J Serb Chem Soc 67(12):867–877
26. Ojani R, Raoof J-B, Afagh PS (2004) Electrocatalytic oxidation of some carbohydrates by poly(1-naphthylamine)/nickel modified carbon paste electrode J Electroanal Chem 571(1):1–8
27. Liu Y (2013) Poly(1-naphthylamine)-nickel modified glassy carbon electrode for electrocatalytic oxidation of formaldehyde in alkaline medium Int J Electrochem Sci 8:4776–4784
28. D'Eramo F, Marioli JM, Arevalo AH, Sereno LE (2003) Optimization of the electrodeposition of copper on poly-1-naphthylamine for the amperometric detection of carbohydrates in HPLC Talanta 61(3):341–352
29. D'Eramo F, Marioli JM, Arevalo AA, Sereno LE (1999) HPLC analysis of carbohydrates with electrochemical detection at a poly-1-naphthylamine=copper Modi@ed electrode Electroanalysis 11(7):481–486
30. Riaz U, Ahmad S, Ashraf SM (2008) Effect of dopant on the nanostructured morphology of poly(1-naphthylamine) synthesized by template free method Nanoscale Res Lett 3(1):45–48
31. Riaz U, Ahmad S, Ashraf SM (2008) Pseudo template synthesis of poly (1-naphthylamine): effect of environment on nanostructured morphology J Nanopart Res 10(7):1209–1214
32. Riaz U, Ahmad S, Ashraf SM (2008) Template polymerization of nano-scale poly(1-naphthylamine): effect of oxidant on the spectral, thermal and morphological characteristics Des Mono Polym 11(2): 201–214
33. Riaz U, Jahan R, Ahmad S, Ashraf SM (2008) Copolymerization of poly(1-naphthylamine) with aniline and o-toluidine J Appl Polym Sci 108(4):2604–2610
34. Massoumi B, Entezami AA, Aghili H (2011) Conductivity and solubility of nanostructure poly (1-naphthylamine-co-aniline) prepared by interfacial polymerization Iran Polym J 20(4):295–303
35. Ashraf SM, Ahmad S, Riaz U (2007) Development of novel conducting composites of linseed-oil-based poly(urethane amide) with nanostructured poly(1-naphthylamine) Polym Int 56(9):1173–1181
36. Ashraf SM, Ahmad S, Riaz U (2006) Synthesis and characterization of novel poly(1-Naphthylamine)-montmorillonite nanocomposites intercalated by emulsion polymerization, J. Macromol. Sci. B, Macromol Phy 45(6):1109–1123
37. Riaz U, Ahmad S, Ashraf SM (2009) Development of novel conducting composites of nanostructured poly(1-naphthylamine) with poly(vinyl chloride) Polym Comp 30(5):528–533
38. Riaz U, Ahmad S, Ashraf SM (2009) Effect of solvent on the characteristics of nanostructured composites of poly (1-naphthylamine) with poly (vinyl alcohol) Curr Appl Phy 9:581–587
39. Radhika S, Murugan KD, Baskaran I, Dhanalakshmi V, Anbarasan R (2009) Metal oxide-assisted chemical synthesis of poly(a-naphthylamine) and characterizations J Mater Sci 44(13):3542–3555
40. Ahmad S, Ashraf SM, Riaz U, Zafar S (2008) Development of novel waterborne poly(1-naphthylamine)/poly(vinylalcohol)-resorcinol formaldehyde-cured corrosion resistant composite coatings Prog Org Coat 62(1):32–39
41. Riaz U, Ahmad SA, Ashraf SM, Ahmad S (2009) Effect of dopant on the corrosion protective performance of environmentally benign nanostructured conducting composite coatings Prog Org Coat 65(3):405–409
42. Riaz U, Ashraf SM (2013) Evaluation of antibacterial activity of nanostructured copolymers of poly (naphthylamine) Int J Polym Mater Polym Biomater 62:406–410
43. Ameen S, Akhtar MS, Kim YS, Yang O-B, Shin H-S (2010) Synthesis and characterization of novel poly(1-naphthylamine)/zinc oxide nanocomposites: application in catalytic degradation of methylene blue dye Coll. Polym Sci 288(16):1633–1638
44. Riaz U, Ashraf SM, Budhiraja V, Aleem S, Kashyap J (2016) Comparative studies of the photocatalytic and microwave-assisted degradation of alizarin red using ZnO/poly(1-naphthylamine) nanohybrids J Mol Liq 216:259–267
45. Riaz U, Ashraf SM (2012) Latent photocatalytic behavior of semi-conducting poly(1-naphthylamine) nanotubes in the degradation of Comassie brilliant blue RG-250 Sep Purf Technol 95:97–102
46. Riaz U, Ashraf SM (2014) Synergistic effect of microwave irradiation and conjugated polymeric catalyst in the facile degradation of dyes RSC Adv 4:47153–47162
47. Riaz U, Ashraf SM, Farooq M (2015) Effect of pH on the microwave-assisted degradation of methyl orange using poly(1-naphthylamine) nanotubes in the absence of UV-visible radiation Coll Polym Sci 293(4):1035–1042
48. Riaz U, Ashraf SM, Ruhela A (2015) Catalytic degradation of orange G under microwave irradiation with a novel nanohybrid catalyst J Environ Chem Engg 3(1):20–29
49. Bagheri H, Daliri R, Roostaie A (2013) A novel magnetic poly(aniline-naphthylamine)-based nanocomposite for micro solid phase extraction of Rhodamine B Anal Chim Acta 794:38–46
50. Tran MT, Nguyen THT, Vu QT, Nguyen MV (2016) Properties of poly(1-naphthylamine)/Fe<sub>3</sub>O<sub>4</sub> composites and arsenic adsorption capacity in wastewater Mater Sci 10(1):56–65